©2012 Allen Institute for Brain Science.

Supplementary Figure 1

Extension of Fig. 1. Anatomical location of HD cells.

a-c: Histology. a: 4',6-Diamidino-2-Phenylindole (Dapi) staining of a thalamic slice. Three electrode tracks are visible in this section. **b**: Fluorescent photograph of PV-YFP showing high-density parvalbumin-immunoreactivity signal in the reticular nucleus of the thalamus. **c**: Merged picture with labeled nuclei. AD, anterodorsal; LD, laterodorsal; AV, anteroventral, AM, anteromedial, MD, mediodorsal; Re, reuniens, RT reticular nucleus. **d-f**: Localization of HD cells. **d**: fraction of HD cells recorded by two adjacent shanks. Session #1 (top squares) corresponds to the first session which detected units in the thalamus. The probe was lowered by 70–140 mm at the end of each session. **e**: Interpolated density of HD cells, based on known inter-shank spacing and the amount of incremental movement of the recording sites between each session. Brightness codes for total number of clustered HD units. **f**: Putative anatomical density of HD cells superimposed on mouse brain atlas (Allen Mouse Brain Atlas. Available from: http://mouse.brain-map.org). **g**: Same as **a** for a slice including the post-subiculum. Arrowheads show four out of the six electrode tracks. PoS: post-subiculum; PRE: pre-subiculum; SUB: subiculum; RSP: retrosplenial cotex; V1: primary visual cortex; SC: superior colliculus. **h**: same as **f** for the animal shown in **g**.
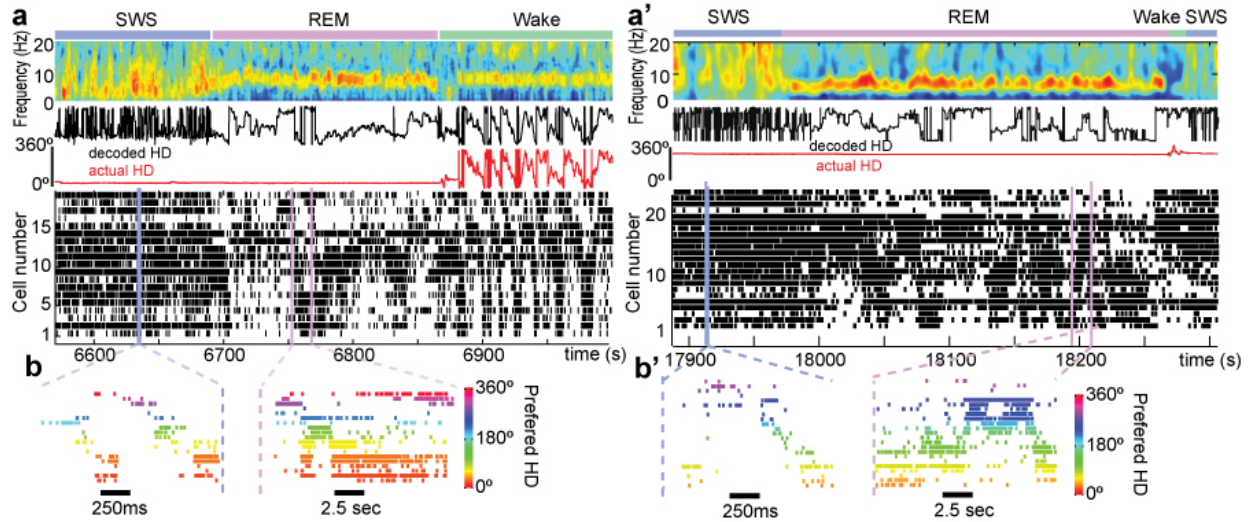
Supplementary Figure 2

Extension of Fig. 1.

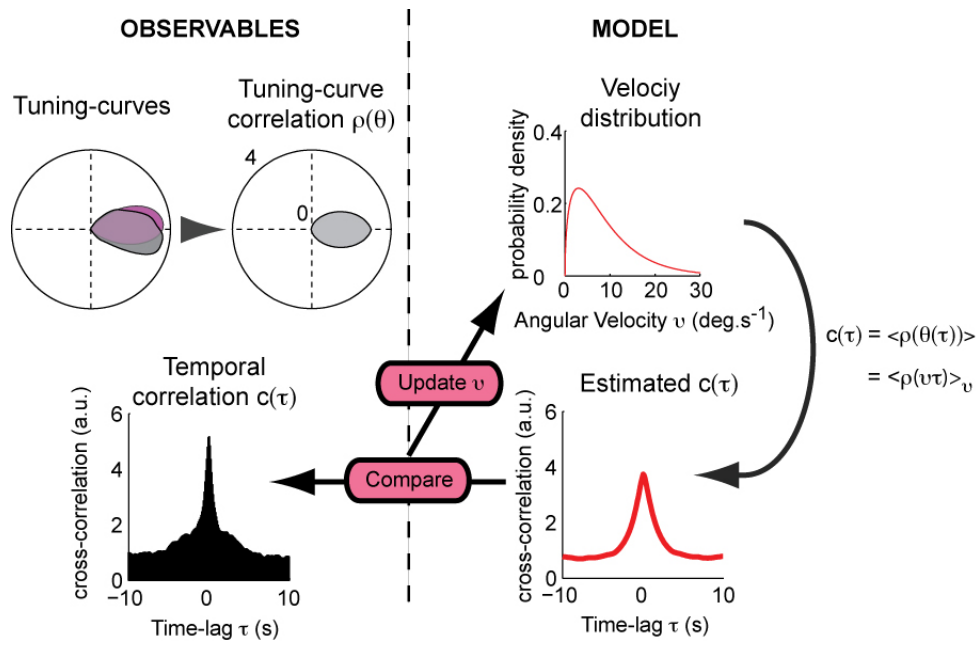**a**: Superimposed tuning curves of ADn (left, n = 242) and PoS (right, n = 111) HD cells, as well as mean tuning curves (colored solid lines). Gray lines, individual HD neurons. 12% of ADn HD cells and 32% of PoS HD cells were not unimodal: their tuning curve showed at least one other peak that was 50% or more than the maximal peak firing rate. **b**: Distribution of peak firing rate for ADn HD cells (red) and PoS HD cells (blue; $p < 10^{-10}$, Mann-Whitney U-test, n = 242 ADn and n = 111 PoS HD cells). **c**: Distribution of cross-validated HD information content for the two populations of cells (same colors as in **b**; $p < 10^{-6}$, Mann-Whitney U-test).

Supplementary Figure 3

Extension of Fig. 1. Two additional examples of thalamic HD cell assembly dynamics across brain states.

a: Top, spectrogram of local field potential recorded from the hippocampal CA1 pyramidal layer. Middle, Bayesian-based decoding (see Methods) of HD signal from the population of ADn HD cells (dark curve) and the animal's actual head orientation (red curve). Bottom, raster plot of 19 simultaneously recorded HD cells sorted by preferred head direction during waking. **b**: Close-up of HD cell population activity during SWS (left) and REM (right). Colors code for preferred head direction during waking. Note orderly changes of unit firing of HD cells in all brain states. Data are from session *m12-120806*. **a'–b'**: same as above for 23 simultaneously recorded HD cells, also in the ADn. Data are from session *m32-140822*.

OBSERVABLES | **MODEL**

Tuning-curves → Tuning-curve correlation $\rho(\theta)$

Velociy distribution

Temporal correlation $c(\tau)$

Estimated $c(\tau)$

Update υ

Compare

$$c(\tau) = \langle\rho(\theta(\tau))\rangle$$
$$= \langle\rho(\upsilon\tau)\rangle_\upsilon$$

Supplementary Figure 4

Illustration of the algorithm used to estimate the head angular velocity from pairwise temporal cross-correlograms of HD cell spike trains.

The angular correlation function is directly inferred from the two tuning curves as the correlation of the firing rates as a function of the angular offset. It is normalized so that 1 represents chance level (as are all other correlations throughout the paper).
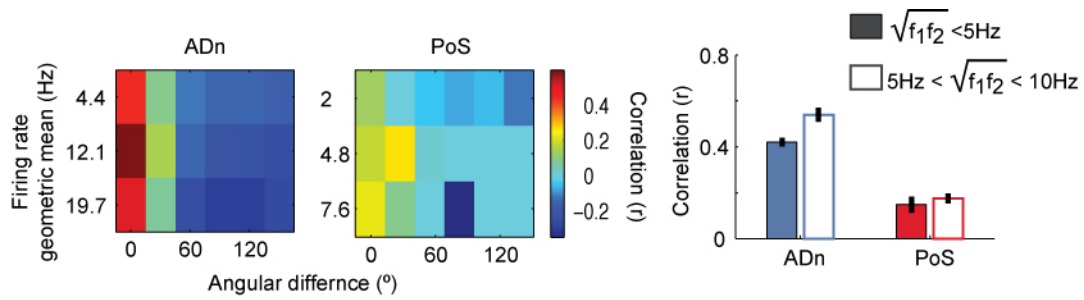
Supplementary Figure 5

Pairwise neuronal correlations were stronger in the ADn than in the PoS, independent of firing rate differences.

Left, average correlations (color-coded) as a function of the difference of preferred directions for increasing value of peak firing rate (geometric mean) in the ADn. Middle, PoS neurons. Right, average (± s.e.m.) correlation for pairs showing firing rate mean <5 Hz (filled bars) or between 5 and 10 Hz (empty bars) in the ADn (left) and the PoS (right). The brain areas comparison effect was significant ($p < 10^{-7}$) but the firing rate group effect was not ($p > 0.05$, two-way ANOVA).
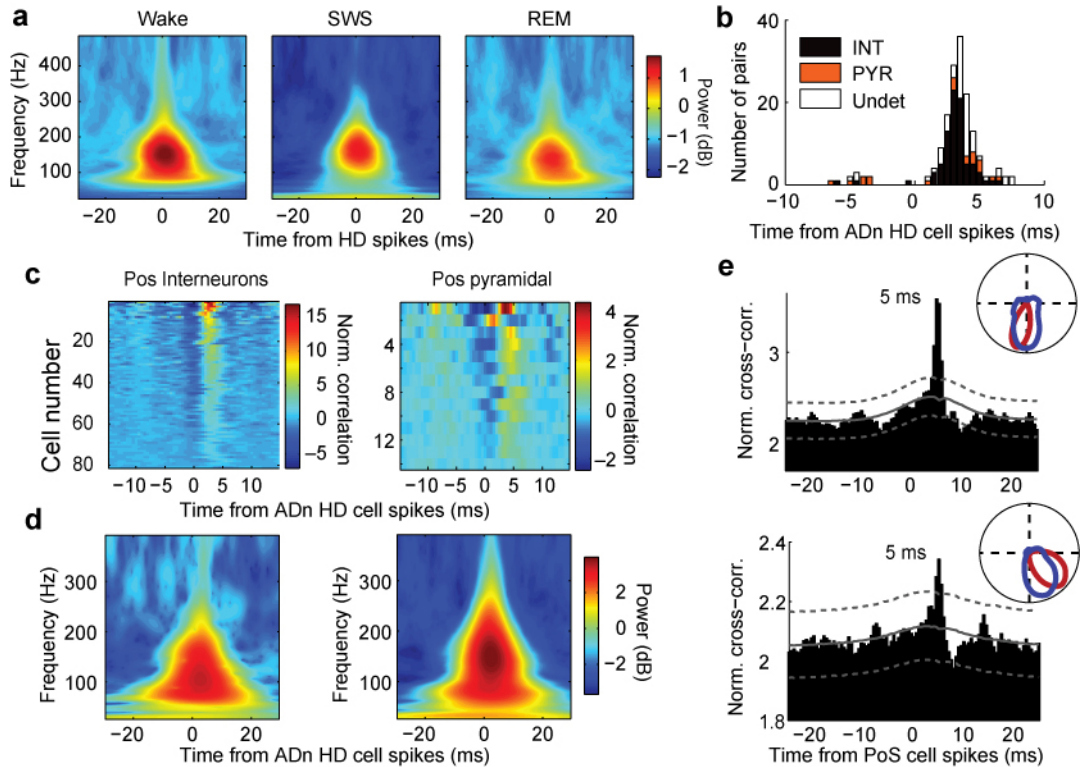
Supplementary Figure 6

Synchronous spiking in the ADn and synaptic recruitment of PoS cells. Separation

a: Average wavelet transform of the ADn-ADn cross-correlograms across brain states. **b**: Histogram of significant cross-correlogram peak times indicates putative mono-synaptic connections between ADn and PoS interneurons (black), pyramidal cells (orange), or undetermined cell types (white). Positive and negative lags correspond to ADn-to-PoS and PoS-to-ADn monosynaptic connections, respectively. **c**: Left, color-coded cross-correlograms between monosynaptically connected ADn HD cell and putative interneurons in the PoS. Right, putative pyramidal cells. **d**: Average wavelet transform of the cross-correlograms shown in **c**. **e**: Two examples of putative monosynaptic connections between PoS HD cells and ADn HD cell targets. Peaks occur at ~5 ms. Insets indicate the HD tuning curves of each neuron (red: ADn, blue: PoS).
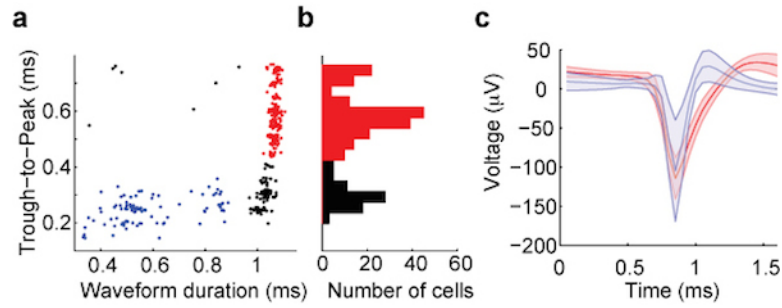
Supplementary Figure 7

Separation between putative pyramidal and interneurons on the basis of waveform features in PoS.

a: Scatter plot of spike duration and trough-to-peak width (see Methods). **b**: Marginal distribution of trough-to-peak width for broad spikes (duration > 0.95ms). The subgroup with short trough-to-peak features was classified as 'undetermined' (black), whereas the rest were classified as putative pyramidal cells (red). **c**: Average waveforms for putative pyramidal cells (red) and interneurons (blue).
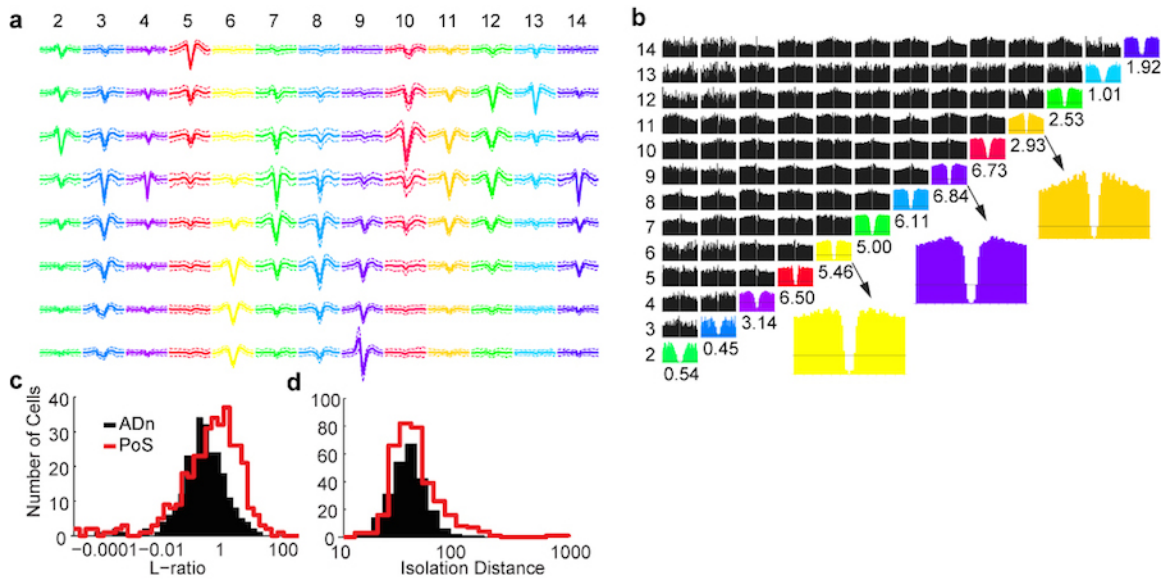
Supplementary Figure 8

Spike sorting and isolation quality of waveform clusters.

a–b: example of 13 ADn units recorded simultaneously (same data as Supplementary Fig. 3; cluster 1 starts at 2 by convention) by one shank of a silicon probe. **a**: Average (± s.d.) of unit waveforms. **b**: Auto-correlograms (in colors) and cross-correlograms (in grey) of all the units. Numbers (and horizontal lines in auto-correlograms) indicate average firing rate. **c**: Distribution of L-ratio measures for ADn (black) and PoS (red) units. **d**: Same as c for the Isolation Distance index.

Animal ID	Hpc wires	ADn probe	PoS probe	# sessions (ADn, ADn+Pos)	# HD cells (total) in ADn	# HD cells (total) in PoS
m12	X	X		5	63 (217)	-
m17	X	X		9	52 (245)	-
m20	X	X		5	15 (49)	-
m24		X	X	(2, 4)	17 (22)	9 (48)
m25		X	X	(3, 10)	23 (27)	53 (135)
m28		X	X	(3, 7)	37 (55)	49 (174)
m32	X	X		2	35 (105)	-

Supplementary Table 1
Summary of physiological recordings.
Total number of recording sessions, of recorded cells and of HD cells in the ADn and/or the PoS, by animals.